J Mater Sci (2008) 43:3960–3968
DOI 10.1007/s10853-007-2137-1

First principles study of the adhesion asymmetry of a metal/oxide interface

C. L. Phillips · P. D. Bristowe

Received: 27 July 2007 / Accepted: 30 August 2007 / Published online: 6 March 2008

Abstract The observed asymmetry in the interfacial adhesion between ZnO and Ag is studied using a first principles density functional approach. The interface formed when ZnO is deposited on Ag (111) is experimentally measured to be stronger than that formed when Ag is deposited on ZnO (0001) and this indicates a possible difference in bonding geometries. It is found that because the ZnO (0001) surface does not exhibit atoms which are onefold coordinated with the sub-surface layer this restricts the way Ag can bond to the surface whereas no such restriction exists, when ZnO is deposited on the Ag (111) surface. The study focuses on a particular Ag (111)/ZnO (0001) interface which has rotated epitaxy and by calculating the ideal work of separation it is found that an O-terminated interface which is onefold coordinated with an adjacent Zn layer is significantly stronger than the corresponding interface which is threefold coordinated with an adjacent Zn layer. This is consistent with the observations, since the onefold coordinated interface cannot form when Ag is deposited on to ZnO (0001). Additional calculations indicate that the stronger onefold coordinated interface can also separate leaving oxygen on the Ag surface provided that surface relaxation effects are suppressed.

Introduction

Interfaces between metals and oxides occur naturally in many fabricated nanostructures used for electronic, magnetic, ferroelectric, superconducting, and optical applications. Examples include MOSFETs, FRAMs, and spin tunnel junctions, where the electronic characteristics of the interface are key to the functionality of the structure. Sometimes, however, the mechanical strength of the interface is equally important particularly in cases where the nanostructure is subject to internal stresses, external load, or chemical corrosion. One such example is the optical multilayer commonly employed to control the flow of thermal energy across glass used for architectural purposes [1]. The functional material in the multilayer is a thin-film of silver which has low-emissivity and consequently reflects infrared radiation [2]. This is the main energy requirement for windows in buildings since it helps reduce solar heating in summer and heat loss in winter [3]. The silver film is necessarily sandwiched between oxide films to protect it and to allow the transmission of visible light through the multilayer. The inherent structure of the multilayer means that there are at least two metal-oxide interfaces present, one closer to the glass substrate than the other. Typically the neighboring oxide is ZnO (or aluminum-doped ZnO) so that the multilayer stack contains the sequence ZnO–Ag–ZnO. All the layers are deposited using magnetron sputtering in a vacuum chamber. The bonding between metals and oxides is known to be relatively weak and is therefore no surprise that under load and/or chemical attack by contaminants from the environment that the interfaces between Ag and ZnO are found to be the weakest in the multilayer [3]. Small regions of the interface are observed to de-laminate and buckle resulting in the appearance of white spots or other flaws on the glass. Furthermore mechanical testing of ZnO–Ag–ZnO multilayers on glass substrates using a wedge-loaded cantilever have shown that the ZnO–Ag interface is about 50% stronger than the Ag–ZnO interface, with a measured

C. L. Phillips · P. D. Bristowe (✉)
Department of Materials Science and Metallurgy,
University of Cambridge, Cambridge CB2 3QZ, UK
e-mail: pdb1000@cus.cam.ac.uk

average value of 2.2 Jm^{-2} for its work of adhesion [4]. It has been proposed that this mechanical asymmetry could be caused by different bonding arrangements at the two interfaces. Different interfacial structures are possible because ZnO lacks a centre of symmetry, has fourfold stacking along the polar direction and can be either oxygen or zinc terminated. However, other factors might contribute to the measured asymmetry such as the presence of interfacial defects, interlayer plasticity and residual stress in the multilayer stack. In the present paper we investigate the strength of the ZnO–Ag–ZnO system using first principles atomistic modeling, focusing specifically on the atomic structure of the ZnO–Ag interface which is found to exhibit a greater range of bonding configurations than the Ag–ZnO interface. First principles calculations on the strength of the Ag–ZnO interface have been described previously [5] and, therefore, direct comparisons between the two variants can be made.

The structure of the ZnO–Ag–ZnO multilayer system

When ZnO is sputtered onto a glass substrate, which is sometimes buffered by another oxide such as TiO_2, a [0001] polar oriented thin-film is formed [6] which is either oxygen or zinc terminated. Theoretical and experimental studies suggest that in O-rich (H-rich) conditions the O-terminated (Zn-terminated) surface is unreconstructed, defect-free and threefold coordinated with the sub-surface layer [7–9]. For simplicity, the present study assumes that these are the prevailing conditions, but it is known that in other chemical environments polar surfaces reconstruct in a variety of ways and can adsorb impurities [10, 11]. The subsequent deposition of Ag onto the ZnO surface produces an interface whose orientation has been determined by electron diffraction [6]. A 30° rotated epitaxial relationship is observed in which $(111)_{Ag} \parallel (0001)_{ZnO}$ and $[110]_{Ag} \parallel [1\bar{1}00]_{ZnO}$ (in the original paper $[1\bar{1}00]_{ZnO}$ was mislabeled as $[11\bar{2}0]_{ZnO}$). This results in a near-coincidence interface with a 2.6% lattice mismatch and is called $(2 \times \sqrt{3})$ *R*30, since two of the shortest lattice vectors in the Ag (111) plane almost match with $\sqrt{3}$ of the shortest lattice vectors in the ZnO (0001) plane. The unrotated epitaxial orientation, called (1×1), in which $[110]_{Ag} \parallel [2\bar{1}\bar{1}0]_{ZnO}$ has an 11% mismatch and has not been observed, probably because of the large misfit strain. This is supported by recent first principles calculations which have shown that the $(2 \times \sqrt{3})$ *R*30 interface is significantly more stable than the unrotated (1×1) interface [5]. These calculations, which employ a threefold coordinated ZnO surface, also indicate that the O-terminated variant of the $(2 \times \sqrt{3})$ *R*30 interface is stronger than the Zn-terminated variant. The calculated strength of the former interface, as determined through the ideal work of separation, is found to be about 1.7 Jm^{-2} if only the interfacial spacing is relaxed and about 1.1 Jm^{-2} if full atomic relaxation is allowed. The corresponding values for the Zn-terminated interface are 1.4 Jm^{-2} and 0.9 Jm^{-2}, respectively. There is no experimental evidence for misfit dislocations at the Ag–ZnO interface probably because the thickness of the Ag film ($\sim$10 nm) is smaller than the critical thickness required for dislocation nucleation [12]. The interface is therefore pseudomorphic and coherent and this is the condition simulated in the above calculations.

Following the deposition of Ag a further layer of ZnO is added to make up the ZnO–Ag–ZnO multilayer sequence. LEED measurements [13] of clean Ag (111) surfaces indicate they are "bulk-like" with (1×1) periodicity and surface normal displacements of <1 Å which are characteristics also reproduced by first principles calculations [14]. Although some surface defects (e.g., vacancies) may to be present prior to the deposition of ZnO (actually Zn in an oxygen-rich environment), the Ag surface is largely ideal and this is the assumption in the present study. The interface formed between ZnO and Ag is likely to exhibit the same orientation relationship as the interface between Ag and ZnO since the lattice mismatch is the same. The Ag film remains compressed by 2.6% over its thickness so that when the ZnO is deposited its takes its bulk lattice parameter. Although the ZnO–Ag and Ag–ZnO interfaces may have the same orientation relationship their interfacial structures may be different locally since the presence of onefold coordinated Zn or O atoms bonded to the Ag surface cannot now be excluded. An oxygen layer, for example, may form first on the Ag surface followed by a zinc layer which is stacked in such a way that the O and Zn layers are onefold coordinated. This would imply that the polarity of the new ZnO layer is the same as that formed at the Ag–ZnO interface which is O-terminated but threefold coordinated. If both interfaces were threefold coordinated then the polarity would be reversed. Possible structures for the onefold coordinated ZnO–Ag interface and threefold coordinated Ag–ZnO interface are shown in Fig. 1. The difference in bonding at the two interfaces may be partly responsible for the observed adhesion asymmetry and this is the focus of the present study.

Computational method

The first principles atomistic modeling is performed using a density functional, plane–wave pseudopotential approach [15], which is implemented in the CASTEP program [16]. The program can optimize the atomic geometry and electronic structure of the metal/oxide interface and calculate its total energy. Ultrasoft pseudopotentials [17] are used for

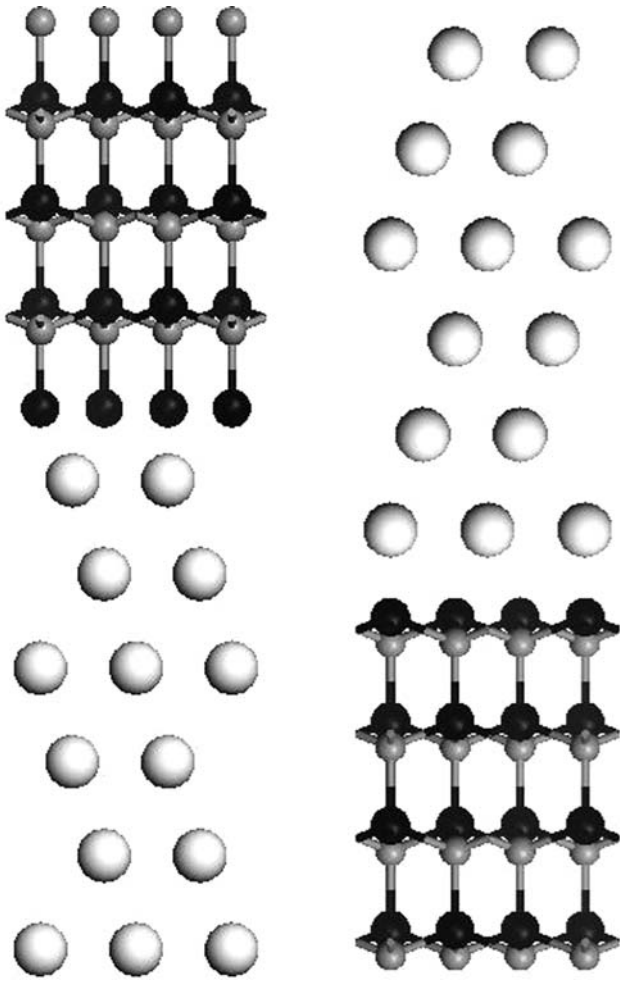

Fig. 1 Possible structures for a onefold coordinated ZnO–Ag interface (left) and a threefold coordinated Ag–ZnO interface (right) in a ZnO–Ag–ZnO multilayer stack. Both interfaces are O-terminated with $(111)_{Ag} \parallel (0001)_{ZnO}$. Small gray, large gray and small black circles are zinc, silver and oxygen atoms, respectively

the electron–ion interactions with the 3*d* and 4*s* electrons for Zn and the 2*s* and 2*p* electrons for oxygen treated as valence electrons. For silver, 4*d* and 5*s* electrons are chosen as the valence electrons. A plane-wave kinetic energy cutoff of 400 eV is employed which is sufficient to achieve convergence to less than 0.02 eV/atom. The generalized-gradient approximation (GGA) with the Perdew, Burke, and Ernzerhof (PBE) exchange-correlation functional is chosen for all the calculations [18]. Monkhorst-Pack *k*-point meshes with a density of at least $(4 \times 4 \times 1)$ points in the Brillouin zone of the primitive ZnO unit cell are used. The initial geometries are optimised by the Broyden, Fletcher, Goldfarb, and Shannon minimiser [19]. The convergence thresholds between optimisation cycles for energy change, maximum force, maximum stress and maximum displacement are set as 10^{-5} eV/atom, 0.03 eV/Å, 0.05 GPa and 0.001 Å respectively. The optimisation terminates when all these criteria are satisfied.

The $(2 \times \sqrt{3})$ *R*30 ZnO–Ag interface is constructed using the supercell method which applies periodic boundary conditions both normal and parallel to the interface. A typical computational cell consists of 6 (111) layers of Ag, 8 (0001) layers of Zn and O, and a 25 Å region of vacuum. The size of the vacuum region is chosen to ensure that the model effectively contains only one interface but in doing so there are, of course, two surfaces present, as well. The ZnO stacking sequence is arranged, so that both ends of the ZnO slab are onefold coordinated. During optimization the surfaces of ZnO and Ag that are exposed to vacuum are held rigid, specifically the three outer layers of ZnO and two outer layers of Ag. Following previous calculations [5] no attempt is made to quench the residual electric field present in the computational slab caused by the polar nature of the oxide. This allows for a direct comparison between the relative strengths of the threefold and onefold coordinated interfaces under the closest possible conditions. Although an approximation this approach is supported by more recent calculations which show that passivating the slab by attaching hydrogen-like atoms to the ZnO surface changes the work of separation of the threefold interface by only 6–7% provided surface relaxation effects are suppressed. As seen later this difference is sufficiently small to allow meaningful comparison between the strengths of the interfaces under these conditions.

In order to optimise the atomic structure of the interface it is necessary to consider its geometrical degrees of freedom. In addition to local relaxations at the interface, the relative displacement or translation state of the ZnO and Ag slabs need to considered as well as the stacking sequences of the two materials. Considering first the stacking sequences, there are twelve possible configurations for onefold coordinated ZnO–Ag interfaces since (0001) ZnO forms an $A\alpha B\beta$ stacking sequence and (111) Ag forms an *abc* stacking sequence. However, previous first principles calculations [5] of the Ag–ZnO interface showed that the important distinction between the configurations in terms of their strength is whether the interface is O or Zn terminated, i.e., *A(B)* or *α(β)* terminated. Therefore, for convenience only two of the stacking configurations are studied in the present work, e.g. *A/a* and *α/a* interfaces. It is straightforward to show that other configurations involving the *b* and *c* Ag layers (e.g., *A/b* or *α/c*) have the same structures as *A/a* and *α/a* but shifted in space. The translational degree of freedom of the interface has two components, one in the plane of the interface and the other normal to the interface. Formally all non-equivalent in-plane translations will fall within the irreducible zone of the pattern conserving or DSC (displacement shift complete) lattice of the $(2 \times \sqrt{3})$ *R*30 coincidence site structure [20]. It is common, however, in atomistic calculations to consider only high-symmetry positions in this zone. Let the reference state be the structure

in which an O plane (or Zn plane) is in coincidence with a Ag atom directly below it. In the literature this has been called the "on-top" site [5, 21]. If the O plane (or Zn plane) is then translated along the sides of the coincidence site unit cell by 1/6[$\bar{1}$10] or 1/6[$\bar{1}$01] relative to the Ag lattice then two further high-symmetry positions are obtained which have been called the "fcc-hollow" and "hcp-hollow" sites, respectively. In the fcc-hollow position there are no coincidences but a Ag atom that lies below the centre of the [0001] channel of the ZnO structure. In the hcp-hollow position coincidences occur only when a second layer (either O or Zn) is deposited. Using these three high-symmetry translation states in combination with the two oxygen or zinc terminated stacking configurations leads to six possible starting structures for the calculations and these are shown in Fig. 2. The out-of-plane translational degree of freedom for each of these structures is applied during the optimization process in what is called "volume relaxation" [5]. During volume relaxation the interface is relaxed only with respect to the interlayer spacing between the ZnO and Ag slabs keeping the in-plane translation state fixed. Once the optimal interlayer spacing has been found, full atomic relaxation is carried out, but with the fixed surface constraints described previously and not allowing the overall supercell dimensions, which include the vacuum region, to change.

In order to determine the strength of the $(2 \times \sqrt{3})$ $R30$ ZnO–Ag interface, the ideal work of separation is determined for each of the six configurations under consideration. The ideal work of separation [22] is the reversible work that would be needed to cleave an interface if diffusion processes and plastic deformation are suppressed and is defined by:

$$W_{\text{sep}} = (E^{\text{Ag}}_{\text{slab}} + E^{\text{ZnO}}_{\text{slab}} - E_{\text{system}})/A \quad (1)$$

where E_{system} is the total energy of the supercell with the ZnO–Ag interface present, $E^{\text{Ag}}_{\text{slab}}$ and $E^{\text{ZnO}}_{\text{slab}}$ are the total energies of the same supercell but with the ZnO (or Ag) layers replaced by vacuum, and A is the area of the interface. It is thus assumed that when separation occurs it takes place between the oxygen layer (if O-terminated, otherwise zinc layer if Zn-terminated) and the silver layer. It is, of course, possible that the interface cleaves along adjacent layers, for example breaking Zn–O bonds and leaving either oxygen or zinc on the Ag surface. One of these cases, in which oxygen is left on the silver surface, is considered in the present study. For the volume relaxed calculations, $E^{\text{Ag}}_{\text{slab}}$ and $E^{\text{ZnO}}_{\text{slab}}$ are determined from isolated bulk slabs which, in the case of Ag, has been compressed in-plane by 2.6%. For the fully relaxed calculations, $E^{\text{Ag}}_{\text{slab}}$ and $E^{\text{ZnO}}_{\text{slab}}$ are determined from isolated relaxed slabs in which the outermost layers are kept fixed as they are when the interface is present.

Results and discussion

Interfacial cleavage which leaves a clean Ag surface

Table 1 lists the calculated optimal interlayer spacings and the ideal works of separation following volume relaxation for the six interfacial configurations. In each case the values correspond to a minimum in the total energy of the system with respect to the distance between the ZnO and Ag slabs. Although these calculations do not allow full atomic relaxation, certain trends are clear: the O-terminated interfaces are more than twice as strong as the Zn-terminated interfaces and within each termination there is little variation in strength with respect to translation state. In addition the interlayer spacings are about 25% shorter for the O-terminated interfaces indicating stronger bonding and again there is not much variation in this length over the translation states. Given these results full atomic relaxation is only performed on one of the six configurations: the O-terminated on-top structure. Following relaxation the work of separation of this interface appears to drop significantly to 0.84 Jm^{-2}. Examination of the total energies and relaxed structures reveal that this drop in strength is dominated by the relaxed energy $E^{\text{ZnO}}_{\text{slab}}$ of the ZnO slab which has oxygen dangling bonds on the surface. The Ag slab, on the other hand, undergoes minimal relaxation as expected. The ZnO surface with dangling bonds is known to be unstable and therefore, not surprisingly, undergoes significant relaxation as shown in Fig. 3. The surface oxygen atoms appear to cluster into groups of three which resembles an ozone-like species but this may be a result of the chosen periodicity of the surface. The relaxed structure of the interface, however, is reliable and, as shown in Fig. 4, exhibits bond length changes of up to 5% normal to the interface.

Since the definition of the ideal work of separation requires the suppression of diffusion processes then the large displacements which occur on the ZnO surface following cleavage should not really be included in the calculation. Thus the work of separation for the O-terminated interface described above was repeated using fixed geometries for the ZnO and Ag slabs taken directly from the relaxed interfacial structure shown in Fig. 4. The resulting strength of the interface using this method, which could be called an *instantaneous* work of separation, is found to be 4.55 Jm^{-2} which illustrates how large an effect the post-separation surface relaxation has. In fact the work of separation is now about 17% larger than that determined solely by volume relaxation, indicating that local relaxation at the interface can strengthen it. In order to compare the strength of this interface to an equivalent threefold coordinated Ag–ZnO interface a similar calculation is performed under identical conditions. In previous work [5], the strength of the O-terminated, threefold coordinated,

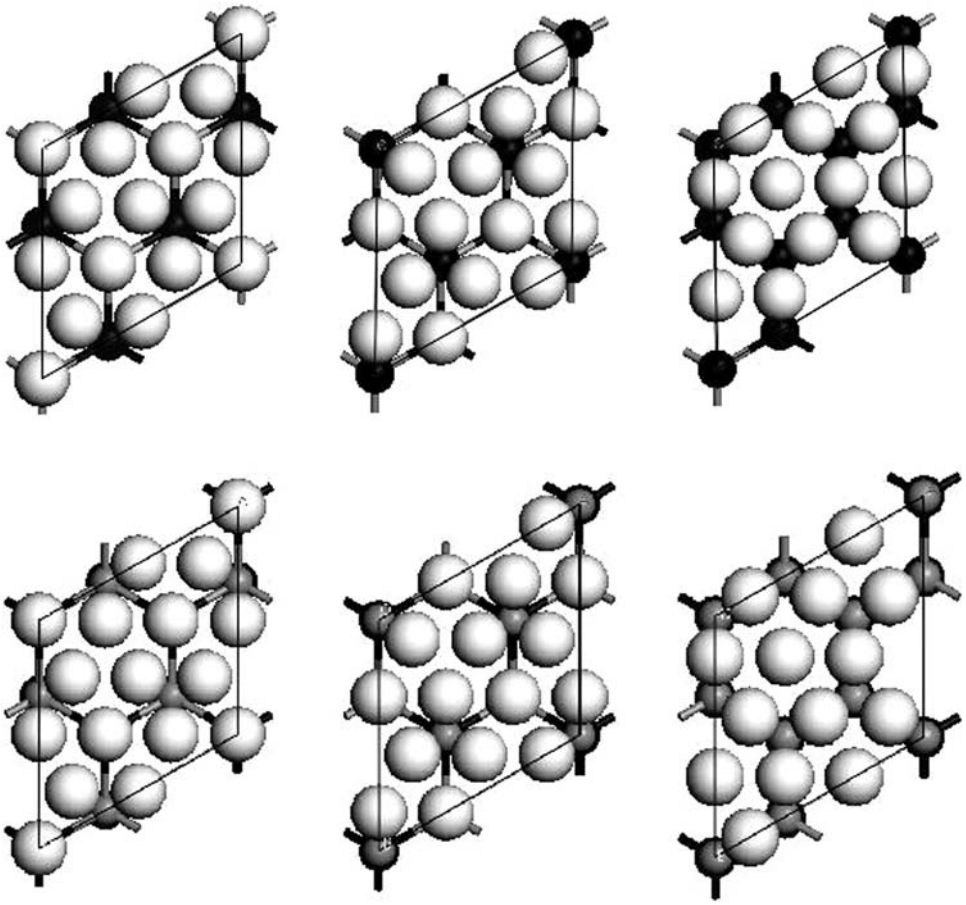

Fig. 2 Plan views of the six starting configurations for the $(2 \times \sqrt{3})$ *R*30 ZnO–Ag interface. Shown in projection are three Ag (111) layers and a double ZnO (0001) layer adjacent to the interface. The rhombuses represent one unit cell in the plane of the interface. The top row are O-terminated at the interface while the bottom row are Zn-terminated. For each termination, from left to right, the translation state is on-top, hcp-hollow and fcc-hollow. Small gray, large gray and small black circles are zinc, silver and oxygen atoms, respectively

Table 1 The volume relaxed interlayer spacings and ideal works of separation for the six O-terminated and Zn-terminated $(2 \times \sqrt{3})$ *R*30 ZnO–Ag interfaces shown in Fig. 2. The cleavage process leaves the Ag surface free of oxygen

	O/Ag interface		Zn/Ag interface	
	d_{O-Ag} (Å)	W_{sep} (Jm^{-2})	d_{Zn-Ag} (Å)	W_{sep} (Jm^{-2})
on-top	1.84	3.89	2.23	1.62
hcp-hollow	1.78	4.06	2.26	1.65
fcc-hollow	1.78	4.05	2.28	1.66

Ag–ZnO interface in the on-top position was found to be 1.70 Jm^{-2} (volume relaxed) and 1.10 Jm^{-2} (fully relaxed). Repeating this calculation but using the ZnO and Ag slabs from the relaxed interfacial structure, a value of 1.49 Jm^{-2} is obtained. This work of separation falls between the values obtained previously, as expected, since the method allows more optimization than volume relaxation but less than full relaxation. Finally, therefore, the relative strengths of onefold and threefold coordinated O-terminated interfaces can be compared under the same computational conditions where it is seen that the onefold ZnO–Ag interface is about three times as strong as the threefold coordinated Ag–ZnO interface (4.55 Jm^{-2} compared to 1.49 Jm^{-2}) which is consistent with the measured asymmetry in the work of adhesion although the calculation predicts that the effect is much stronger.

Interfacial cleavage which leaves an oxygen covered Ag surface

It is possible that when the interface cleaves some oxygen or zinc is left on the Ag surface. To determine whether this process is energetically preferred over the process considered above in which the Ag surface remained oxygen-free following separation, a further set of calculations are performed focusing on the O-terminated interface which results, after cleavage, in an oxygen covered Ag surface. Clearly this process would not leave onefold coordinated oxygen atoms on the ZnO surface and hence could be more favorable. Firstly, volume relaxed results are obtained using the method described in Section "Interfacial cleavage which leaves a clean Ag surface". The ZnO slab is now oxygen deficient and is terminated by Zn atoms at both ends, one group onefold coordinated and the other threefold coordinated with the sub-surface layers. The Ag slab has ¾ ML of oxygen atoms on one surface and these atoms

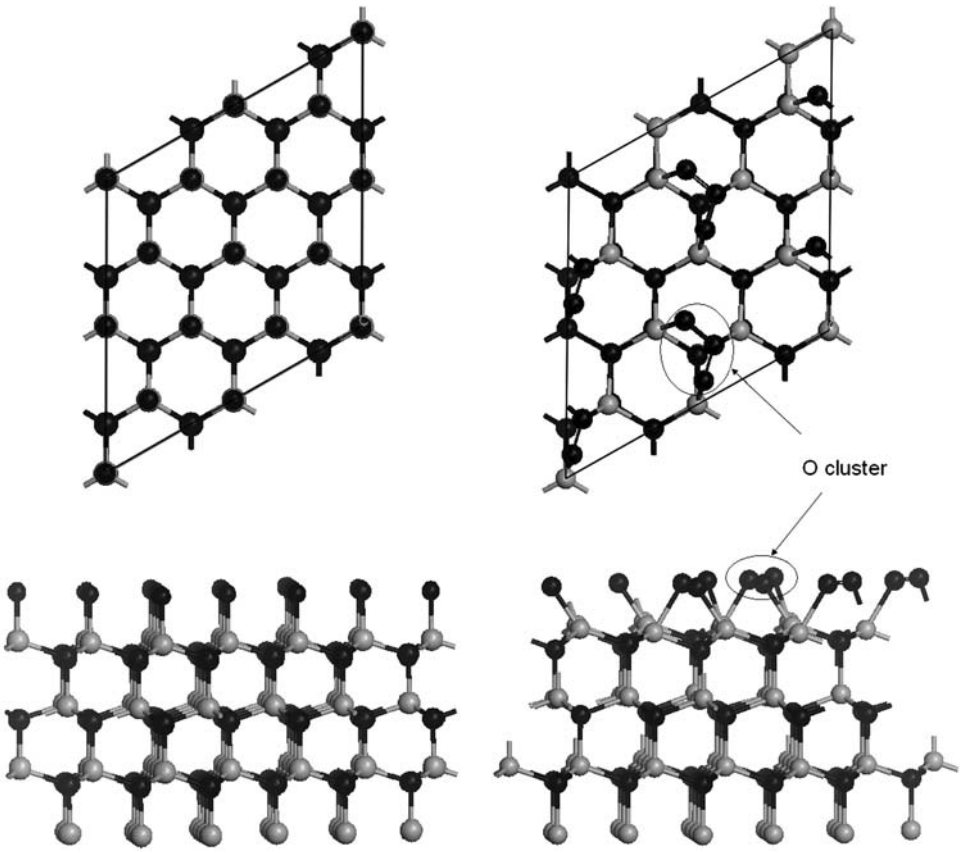

Fig. 3 Plan and side views of the O-terminated ZnO slab before (left) and after (right) relaxation. The rhombuses represent four unit cells on the surface in same orientation as the $(2 \times \sqrt{3})$ *R*30 interface. Surface oxygen atoms relax to form small clusters. Small gray and black circles are zinc and oxygen atoms, respectively

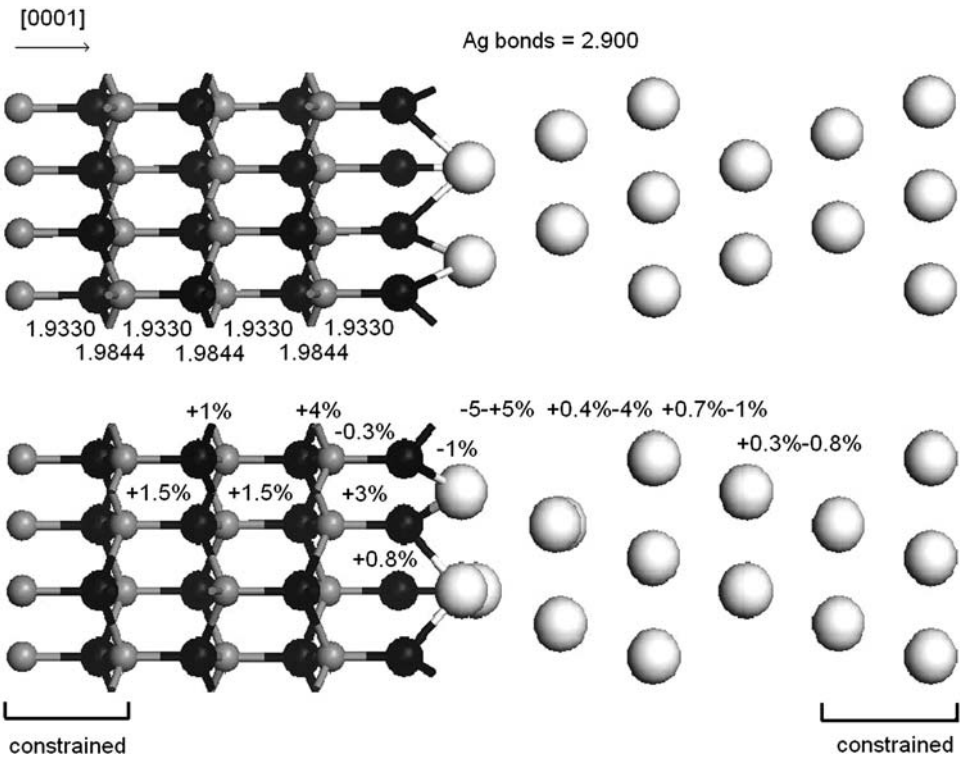

Fig. 4 Side views of the unrelaxed (top) and relaxed (bottom) structures of the O-terminated $(2 \times \sqrt{3})$ *R*30 ZnO–Ag interface in the on-top translation state. The unrelaxed structure gives the starting bond lengths (Å) and the relaxed structure gives the percentage changes after optimization. Small gray, large gray and small black circles are zinc, silver and oxygen atoms, respectively

are arranged in the three high-symmetry configurations. The total energies of the interfaces and their interlayer spacings remain the same as determined in Section "Interfacial cleavage which leaves a clean Ag surface". The results are shown in Table 2 where it is seen that cleaving the interface in this way is comparable to

Table 2 The volume relaxed interlayer spacings and ideal works of separation for the three O-terminated ($2 \times \sqrt{3}$) *R*30 ZnO–Ag interfaces shown in Fig. 2. The cleavage process leaves a ¾ ML of oxygen on the Ag surface

	O/Ag interface	
	d_{O-Ag} (Å)	W_{sep} (Jm^{-2})
on-top	1.84	4.33
hcp-hollow	1.78	4.32
fcc-hollow	1.78	4.32

retaining a clean Ag surface since the works of separation averaged over the translation states in both cases are similar (4.00 Jm^{-2} compared to 4.32 Jm^{-2}).

Following the approach described in Section "Interfacial cleavage which leaves a clean Ag surface" full relaxation is performed on only one of the three configurations listed in Table 2: the O-terminated on-top structure. After relaxation the work of separation of this interface decreases to 2.31 Jm^{-2}. Again the relaxed energies and structures are examined and this time it is the oxygen covered Ag slab that undergoes significant relaxation as shown in Fig. 5. There are three oxygen atoms per unit surface area and two of them are seen to dimerise. Previously conducted density functional calculations of ¾ ML covered Ag (111) surfaces did not report this effect possibly because their initial distribution of Ag atoms on the surface was more symmetric, i.e., always over equivalent sites [23]. If surface relaxation is suppressed using the method described before then the work of separation becomes 4.35 Jm^{-2}. This can be compared to the corresponding result for the cleavage process that leaves the Ag surface oxygen-free and is again found to be similar (4.35 Jm^{-2} compared to 4.55 Jm^{-2}). Thus, as was the case for volume relaxation, it is energetically possible for cleavage to occur with or without leaving oxygen on the

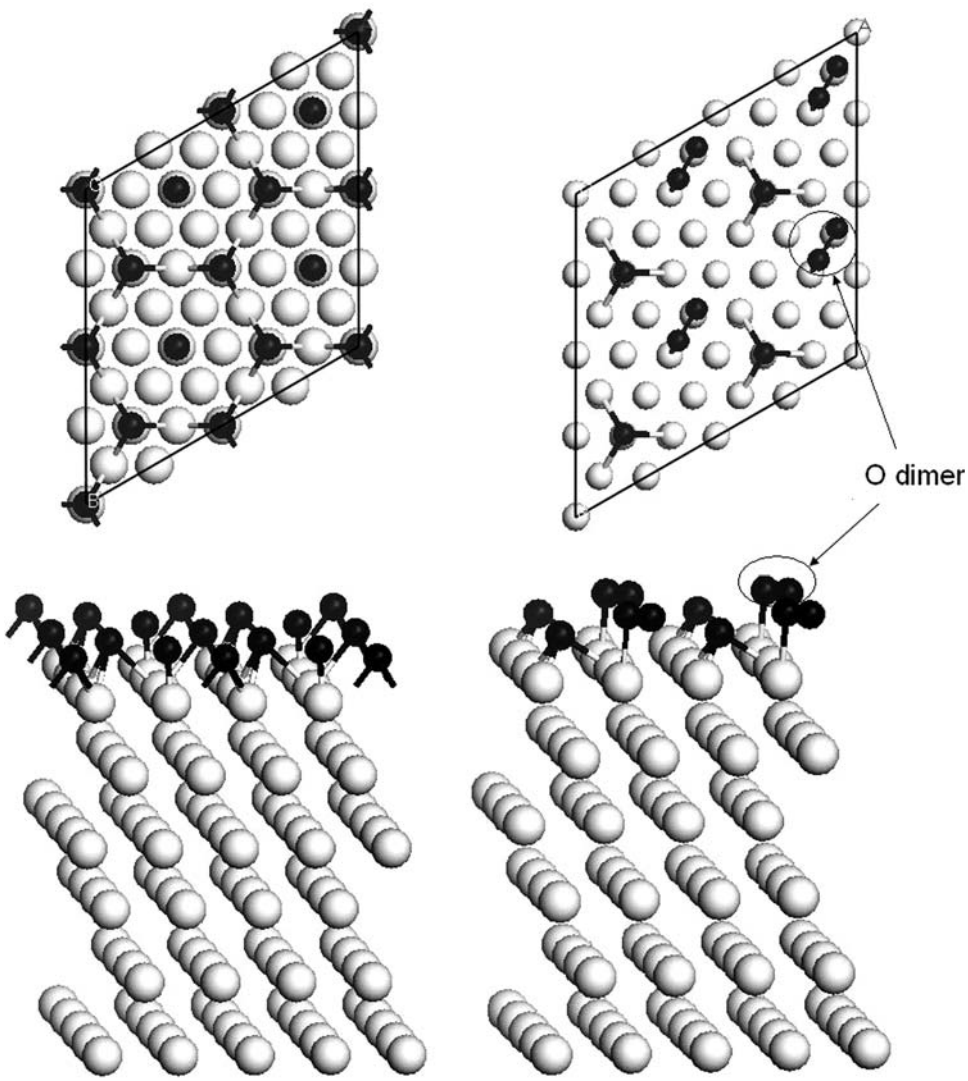

Fig. 5 Plan and perspective views of the oxygen covered Ag slab before (left) and after (right) relaxation. Some surface oxygen atoms reconstruct to form dimers, others remain above hollow positions on the surface. Large gray and small black circles are silver and oxygen atoms, respectively

Table 3 The instantaneous and fully relaxed ideal works of separation (Jm^{-2}) for the on-top O-terminated ($2 \times \sqrt{3}$) *R*30 ZnO–Ag interface which is threefold coordinated (3-c), onefold coordinated (1-c) and onefold coordinated leaving oxygen on the Ag surface (1-c-O)

	O/Ag interface		
	3-c	1-c	1-c-O
Full relaxation	1.10	0.84	2.31
Instantaneous relaxation	1.49	4.55	4.35

Ag surface. The fully relaxed and instantaneous works of separation for the different processes are summarised in Table 3.

Conclusions

The sequential deposition of a ZnO–Ag–ZnO multilayer thin-film stack can result in different atomic structures at the two metal/oxide interfaces. It is proposed that this could be a contributing factor in the observed mechanical asymmetry of the stack. It is recognized, however, that other properties of the stack such as residual stress and interfacial defects will play a role and still need to be investigated. The different structures of the interfaces originate in the non-centric crystallography of ZnO and the local coordination at the ZnO polar surface. When Ag is deposited onto a ZnO (0001) surface it bonds with atoms, either O or Zn, which are threefold coordinated with the sub-surface layer. The absence of onefold coordination restricts the local bonding environment. However, when ZnO is deposited onto a Ag (111) surface, the O or Zn atoms can attach to the surface in such a way as to be either onefold or threefold coordinated to the subsequent ZnO layer that forms. In other words the stacking sequence is not restricted and the polarity of the crystal can be reversed. Consider, for example, a multilayer in which the Ag–ZnO interface is O-terminated and threefold coordinated with [0001] ZnO polarity. Then the ZnO–Ag interface could also have O-termination and be either onefold coordinated with the same polarity or threefold coordinated with $[000\bar{1}]$ polarity. Alternatively it could have Zn-termination and be either threefold coordinated with the same polarity or onefold coordinated with $[000\bar{1}]$ polarity. Previous calculations [5], which were limited to threefold coordinated geometries, indicated that the O-terminated interface was slightly stronger than the Zn-terminated interface (1.1 vs. 0.9 Jm^{-2} for the fully relaxed work of separation). Thus if the ZnO–Ag and Ag–ZnO interfaces are both threefold coordinated with the latter being O-terminated then there is a predicted 18% adhesion asymmetry. While this is consistent with the measurements, the asymmetry is somewhat weaker than observed. The present calculations, which have focused on onefold coordinated geometries, also show that the O-terminated variant is stronger. However, given the restricted coordination at the Ag–ZnO interface, the relative strengths of threefold and onefold geometries need to be determined. Given the large relaxations that can occur at ZnO surfaces with onefold coordinated oxygen atoms, only the instantaneous works of separation can be compared reliably. The calculations show when the ZnO–Ag interface is O-terminated and onefold coordinated it is significantly stronger than the Ag–ZnO interface when it is also O-terminated, but threefold coordinated (4.55 Jm^{-2} compared to 1.49 Jm^{-2}). The predicted adhesion asymmetry is now strong and unequivocal leading to the conclusion that differences in the atomic structures of the two interfaces in a ZnO–Ag–ZnO multilayer stack must contribute to its mechanical properties. Of course regions of onefold and threefold coordination could co-exist in the ZnO–Ag interface (separated by antiphase boundaries) but there would still be a significant adhesion asymmetry. Finally, the study shows that when the onefold coordinated O-terminated ZnO–Ag interface cleaves it can do so with or without leaving a layer of oxygen on the Ag (111) surface, implying that the Zn–O and Ag–O bonds have approximately the same strength. However, this result may depend on the amount of oxygen that remains on the Ag surface (¾ ML is assumed here) and the degree to which it can diffuse into the Ag sub-surface layers. Some chemical mixing at the interface is known to occur (Ag into ZnO, and O into Ag) and the effects of this inter-diffusion on the strength of the interface is the subject of future investigations.

Acknowledgements Funding for this study was provided by EPSRC and the calculations were performed using high performance computing facilities at the University of Cambridge and at the Daresbury Laboratory. The authors would like to thank Zheshuai Lin, Steve Bull, Jinju Chen, Paul Warren and John Ridealgh for useful discussions. The work forms part of a UK Materials Modelling Consortium on Functional Coatings.

References

1. Glaser HJ (2000) Large area glass coating. Von Ardenne Anlagentechnik, Gmbh, Dresden
2. Hummel RE, Guenther KH (eds) (1995) Handbook of optical properties: thin films for optical coatings, vol 1. CRC, Boca Raton
3. Ridealgh JA (2006) Mat Res Soc Proc 890:39
4. Barthel E, Kerjan O, Nael P, Nadaud N (2005) Thin Solid Films 473:272
5. Lin Z, Bristowe PD (2007) Phys Rev B 75:205423
6. Arbab M (2001) Thin Solid Films 381:15
7. Wander A, Schedin F, Steadman P, Norris A, McGrath R, Turner TS, Thornton G, Harrison NM (2001) Phys Rev Lett 86:3811
8. Meyer B, Marx D (2003) Phys Rev B 67:035403
9. Meyer B (2004) Phys Rev B 69:045416

10. Kunat M, Gil Girol St, Becker Th, Burghaus U, Woll Ch (2002) Phys Rev B 66:081402
11. Kresse G, Dulub O, Diebold U (2003) Phys Rev B 68:245409
12. Matthews JW, Blakeslee AE (1974) J Cryst Growth 27:118
13. Culbertson RJ, Feldman LC, Silverman PJ, Boehm H (1981) Phys Rev Lett 47:657
14. de Leeuw NH, Nelson CJ (2003) J Phys Chem B 107:3528
15. Payne MC, Teter MP, Allan DC, Arias TA, Joannopoulos JD (1992) Rev Mod Phys 64:1045
16. Clark SJ, Segall MD, Pickard CJ, Hasnip PJ, Probert MJ, Refson K, Payne MC (2005) Z Kristallogr 220:567
17. Vanderbilt D (1990) Phys Rev B 41:7892
18. Perdew JP, Burke K, Ernzerhof M (1996) Phys Rev Lett 77:3865
19. Fischer TH, Almlof J (1992) J Phys Chem 96:9768
20. Tarnow E, Dallot P, Bristowe PD, Joannopoulos JD, Francis GP, Payne MC (1990) Phys Rev B 42:3644
21. Meyer B, Marx D (2004) Phys Rev B 69:235420
22. Finnis MW (1996) J Phys: Condens Matter 8:5811
23. Li WX, Stampfl C, Scheffler M (2002) Phys Rev B 65:075407